Saudi Pharmaceutical Journal 31 (2023) 1125–1138

HOSTED BY

Contents lists available at ScienceDirect

Saudi Pharmaceutical Journal

journal homepage: www.sciencedirect.com

Original article

Bioinformatics and network pharmacology-based study to elucidate the multi-target pharmacological mechanism of the indigenous plants of Medina valley in treating HCV-related hepatocellular carcinoma

Mubarak A. Alamri

Department of Pharmaceutical Chemistry, College of Pharmacy, Prince Sattam Bin Abdulaziz University, Al-Kharj 16278, Saudi Arabia

ARTICLE INFO

Article history:
Received 4 March 2023
Accepted 3 April 2023
Available online 10 April 2023

Keywords:
Indigenous plants
Medina valley
Multi-target approach
Network pharmacology
HCV-related HCC
Active compounds
Molecular docking

ABSTRACT

The incidence of Hepatocellular Carcinoma (HCC) in Saudi Arabia is not surprising given the relatively high prevalence of hepatitis C virus (HCV) infection. Hepatitis C is also common in Saudi Arabia with a prevalence rate of 1% to 3% of the population, which further increases the risk of HCC. The incidence of HCC has been increasing in recent years, with HCV-related HCC accounting for a significant proportion of cases. Traditional medicine has long been a part of Saudi Arabian culture, and many medicinal plants have been used for centuries to treat various ailments, including cancer. Following that, this study combines network pharmacology with bioinformatics approaches to potentially revolutionize HCV-related HCC treatment by identifying effective phytochemicals of indigenous plants of Medina valley. Eight indigenous plants including *Rumex vesicarius, Withania somnifera, Rhazya stricta, Heliotropium arbainense, Asphodelus fistulosus, Pulicaria incise, Commicarpus grandiflorus,* and *Senna alexandrina,* were selected for the initial screening of potential drug-like compounds. At first, the information related to active compounds of eight indigenous plants was retrieved from public databases and through literature review which was later combined with differentially expressed genes (DEGs) obtained through microarray datasets. Later, a compound-target genes-disease network was constructed which uncovered that kaempferol, rhazimol, beta-sitosterol, 12-Hydroxy-3-keto-bisnor-4-cholenic acid, 5-O-caffeoylquinic acid, 24-Methyldesmosterol, stigmasterone, fucosterol, and withanolide_J decisively contributed to the cell growth and proliferation by affecting ALB and PTGS2 proteins. Moreover, the molecular docking and Molecular Dynamic (MD) simulation of 20 ns well complemented the binding affinity of the compound and revealed strong stability of predicted compounds at the docked site. But the findings were not validated in actual patients, so further investigation is needed to confirm the potential use of selected medicinal plants towards HCV-related HC.

1. Introduction

Hepatocellular carcinoma (HCC) is the predominant type of primary liver cancer, representing 70 to 85% of cases globally (Magalhães et al., 2023). HCC typically arises from underlying liver disease, including chronic infections with hepatitis B virus (HBV) or hepatitis C viruses (HCV), and cirrhosis (Suresh et al., 2020). In its early stages, HCC is often asymptomatic, making it challenging to diagnose and treat effectively. As a result, HCC exhibits a significant fatality rate, thus emphasizing the significance of prompt identification and preventive measures to enhance clinical prognosis for minimizing the worldwide incidence of liver cancer (Qu et al., 2019). HCV is identified as the principal risk element for HCC in Saudi Arabia (Poustchi et al., 2010). In general, 40% of HCC patients in Saudi Arabia were attributed to HCV, whereas 35% of cases were associated with HBV (Alavian and Haghbin, 2016). The primary factors contributing to HCC development in chronic HCV infection include comorbid liver diseases, viral genotype, lifestyle factors, and the co-occurrence of diabetes mellitus (Goossens and Negro, 2014). Co-occurrence of diabetes, comorbid liver diseases, and genotype of the virus greatly contribute to HCC development in HCV infection. Based on available data, persons with obesity have 1.5 to 4-fold greater likelihood of develop-

Peer review under responsibility of King Saud University.

Production and hosting by Elsevier

E-mail address: m.alamri@psau.edu.sa

https://doi.org/10.1016/j.jsps.2023.04.003
1319-0164/

ing HCC as compared to individuals without obesity (Marrero et al., 2005). Most importantly, multiple treatment options are available which are intended to eradicate the viral infections, lowering the transmission rate to others, and reducing the probability of developing HCC (Smith et al., 2012). Despite that, the morbidity rate of affected individuals remains high and available drugs do not produce satisfactory results. Therefore, the limited treatment options and high mortality rate of HCV-related HCC have attracted the great attention of researchers from all over the world. Thus, the implementation of pharmacological treatment comprising natural agents is deemed a feasible therapeutic approach for HCV-related HCC, and could potentially offer solutions to the queries raised previously.

The floral biodiversity of Saudi Arabia comprises approximately 2250 species, which are distributed throughout the Kingdom (Rahman et al., 2004). Saudi Arabia is renowned for its diverse array of cultivated as well as wild cultivated flora (Sher et al., 2010). Unfortunately, the intergenerational transfer of indigenous knowledge is impeded by several factors, including limited information dissemination and a scarcity of data on their practical applications, as well as difficulties in identifying wild medicinal plants. These challenges hinder the preservation and utilization of traditional knowledge, posing a threat to cultural heritage and potential therapeutic resources. Recently, Alsaedi et al. (Alsaedi and Aljeddani, 2022) screened *Rumex vesicarius, Withania somnifera, Rhazya stricta, Heliotropium arbainense, Asphodelus fistulosus, Pulicaria incise, Commicarpus grandiflorus,* and *Senna alexandrina,* as a source of herbal remedies in Medina valley. These plants are used by people inhabiting in these areas for treatment of various ailments, however, the underlying action mechanism of these plants for treating diseases and disorders is completely unknown.

Sensing the opportunities provided by active compounds, Hopkin (Hopkins, 2007) developed an integrative *in silico* approach "network pharmacology" which shifted the paradigm from 'one drug-one target' to a 'multiple-target model. Network pharmacology has now proved to be a boon in the drug-designing process as it assists in the rebirth of indigenous knowledge (Chandran et al., 2017). This approach serves as a benchmark for the initial screening of active ingredients and identification of novel therapeutic targets to better understand the pathophysiology of disease (Noor et al., 2022). Hence, it inevitably contributes to the globalization and modernization of botanical herbs and brings about a paradigm shift in the drug discovery process. In short, the path to the successful discovery of candidate drugs frequently demands an understanding of the complicated network pharmacology landscape.

This study is attributed to the identification of active ingredients, corresponding targets, and multi-target pharmacological mechanisms of the anti-HCC effect of *Rumex vesicarius, Withania somnifera, Rhazya stricta, Heliotropium arbainense, Asphodelus fistulosus, Pulicaria incise, Commicarpus grandiflorus,* and *Senna alexandrina,* by integrating network pharmacology with bioinformatics approaches. Network pharmacology constructs multi-component and multitarget models to clarify the complex interactions between active compounds and target proteins from a network perspective. Molecular docking studies were added as a supplement to validate the results. Afterward, the interaction mechanism, stability, and conformational changes of docked complexes were analyzed by performing molecular dynamic (MD) simulation at 20 ns. To our knowledge, this study is the first to explore the efficacy and mechanism of indigenous plants of Medina valley for treating HCV-related HCC, as well as providing theoretical support and directions for further basic research.

2. Materials and methods

2.1. Data preparation

2.1.1. Active compounds database building

All components of the 8 indigenous plants of Medina valley were collected from literature as well as publically available repositories including KNApSAcK (Nakamura et al., 2013), and Indian Medicinal Plants, Phyto-chemistry Additionally, Therapeutics (IMPPAT) (Mohanraj et al., 2018) databases. "*Asphodelus fistulosus*", "*Commicarpus grandifloras*", "*Heliotropium arbainense*", "*Pulicaria incisa*", "*Rhazya stricta*", "*Rumex vesicarius*", "*Senna alexandrina*", and "*Withania somnifera*" were used as plant-specific keywords in KNApSAcK, IMPPAT, and TCMSP databases, while review of existing literature was performed using the online platforms Google Scholar and PubMed. After retrieval of phytochemicals, the compound with drug-like potential was screened based on their Drug likeness (DL) and Oral Bioavailability (OB). OB refers to the fraction of a drug or compound that reaches the systemic circulation following oral administration and is available to exert its intended pharmacological effects. An OB $\geq$ 30% is considered a commonly used criterion for the screening of compounds because it suggests that a significant proportion of the orally administered drug or compound can be absorbed and reach systemic circulation. A compound with an OB value of<30% may have limited efficacy as it is poorly absorbed and may require higher doses to achieve therapeutic effects. Therefore, a higher OB value increases the likelihood of a compound being effective and therefore, is thought to be an important variable in drug development as well as its optimization. Similarly, the qualitative assessment of a molecule's likelihood to become an oral drug based on its bioavailability is evaluated through DL analysis. Only those active compounds which met the threshold value of OB $\geq$ 0.30 and DL $\geq$ 0.18 were selected as putative compounds with drug-like potential. Following that SwissADME and MolSoft tools were employed to predict the DL and OB of retrieved compounds.

2.1.2. ADMET profiling

While OB and DL are important factors to consider when evaluating the drug-like potential of compound, however, these parameters are not the only factors that determine the effectiveness of compounds for further development. Other important parameters, including absorption, distribution, metabolism, excretion, and toxicity (ADMET) properties, also need to be evaluated to determine whether a compound has the potential to be an effective and safe drug. ADMET properties are assessed during the early stages of drug development and are critical in predicting a drug's potential efficacy, safety, and pharmacokinetics. The goal of ADMET profiling is to optimize the pharmacological properties of a drug candidate and reduce the likelihood of failure during clinical trials. Regarding this, SwissADME server (Daina et al., 2017) and Protox II (Banerjee et al., 2018) tool were used to check the ADMET properties of selected ingredients. Active ingredients with better absorption, inactive toxicity, and good solubility features were considered for subsequent analysis.

2.1.3. Prediction of compound-related targets

The integrative efficacy of compounds of the 8 indigenous plants of Medina valley was determined by analyzing the interaction obtained from two different platforms including STITCH (Gfeller et al., 2014) and Swiss Target Prediction (Kuhn et al., 2007) databases, with the species limited as "*Homo sapiens*". In the case of the STITCH database, only those targets with a combined score greater than or equal to 0.7 were chosen for further analysis. While the SMILES of selected ingredients were subjected

to Swiss Target Prediction to identify the potential targets based on the reverse pharmacophore matching approach. Regarding this, only those target proteins having a probability value greater ≥ 0.7 were selected as the potential targets of 8 indigenous plants.

2.1.4. Microarray data analysis for identification of disease-related target

In current work, the microarray data utilized were sourced from the publicly accessible Gene Expression Omnibus (GEO) database, which is hosted by NCBI of the United States (Clough and Barrett, 2016). The HCV-related HCC was used as a search term in the NCBI-GEO database and three microarray datasets including GSE107170, GSE69715, and GSE62232 were retrieved (Table 1). The microarray datasets were selected based on the criteria that the datasets must include tissue samples from both diseased liver tissues and normal liver tissues. Further, each dataset consisted of more than three samples. The microarray data were then processed using the Limma package of R for the identification of Differentially Expressed Genes (DEGs) which were then considered disease-related targets of HCV-related HCC.

2.2. Compound-target network construction

After the identification of putative targets of both disease and plants, a venn plot was constructed for the identification of overlapped genes between plants and HCV-related HCC. These overlapped genes were then considered as the potential targets of indigenous plants of Medina valley which can be considered as the potential biomarkers to halt the pathophysiology of HCV-related HCC. Further, Cytoscape version 3.8 was used for the construction of a compound-target network (Shannon et al., 2003) based on the overlapped genes. In the compound-target network, the nodes symbolize the ingredients and their associated proteins while the solid black lines denote the interaction that exist among target proteins and compounds. Lastly, the network-analyzer was used to assess the degree of connectivity of compounds within compound-target network.

2.3. Functional annotation of overlapped genes

After the successful identification of overlapped genes, the Gene Ontology (GO) and pathway enrichment analyses were employed for unveiling their underlying molecular functions (MF), biological processes (BP), cellular components (CC), and key signaling pathways. The BP category describes the biological processes in which a gene or protein is involved, the CC category describes the subcellular locations where a gene or protein is active, and the MF category describes the specific molecular activities and interactions in which a gene or protein is involved. In this regard, the Database for annotation, visualization, and integrated discovery (DAVID) (Dennis et al., 2003) was employed for the functional annotation of overlapped targets. DAVID database yielded several GO terms and KEGG pathways, but the threshold of p-value<0.05 was set for screening of statistically significant KEGG pathways and GO terms. Lastly, the ggplot2 package of R was used for the visualization of the top 20 GO terms and top 20 KEGG pathways based on their count and p-value < 0.05.

2.4. Protein-Protein interaction (PPI) network construction

Following the identification of the common genes, they were inputted into the STRING database to generate PPI network (Von Mering et al., 2005). PPIs are remarkably significant due to their high specificity, adaptability, and versatility. The functional interactions between the overlapping targets were assessed based on a combined score threshold of 0.4. The resulting PPI network was then subjected to Cytoscape version 3.8 (Shannon et al., 2003) for the identification of hub genes. Hub genes are highly connected nodes with multiple interactions with other proteins. Hub genes are considered critical components of the PPI network as they have a key role to play in maintaining the integrity and stability of the network, and they are often associated with key biological processes and pathways. Hub genes are usually identified by analyzing the topology of the PPI network, using measures such as degree, betweenness, or closeness centrality. In current study, degree methods available in CytoHubba was used for the selection of hub genes.

2.5. Compound-target-disease network construction

To further explore the action mechanism of native plants on HCV-related HCC, the active ingredients-target protein and target protein-disease networks were constructed through Cytoscape version 3.8. (Shannon et al., 2003). These networks were than merged to construct a final compound-target-disease network. In network, the nodes symbolize the disease related pathway, compounds, and proteins, while the interaction between these nodes were indicated with solid lines. This integrated network provides valuable insights about the synergistic effect of compounds when these plants were used for treating HCV-related HCC.

2.6. Molecular docking analysis

To validate the accuracy of the network pharmacology prediction, molecular docking analysis was employed to confirm the interactions among key targets and compounds. This enables the identification of potential drug combinations that may have synergistic effects on disease treatment. In the current study, Autodock vina 1.1.2 in PyRx 0.8 (Dallakyan and Olson, 2015) was employed for docking analysis of the predicted X-ray crystal structure of hub proteins against active ingredients. The SDF formats of compounds were downloaded from PubChem data, and were exposed to OpenBabel, available in PyRX for energy minimization. In order to achieve a stable conformation, an optimization algorithm known as conjugate gradient descent was utilized in conjunction with the Universal Force Field (UFF) as the energy minimization parameter. Further, 2000 steps were set for energy minimization and the minimization was set to stop at an energy difference of < 0.01 kcal/mol. The energy-minimized ligands were converted to.pdbqt format docking. Later, binding pockets of target proteins were found by utilizing an online CASTp tool. (Tian et al., 2018). Later, the target docking approach was used in PyRx 0.8

Table 1
Brief description of microarray datasets used in the current study.

GEO datasets	Sample	Disease	Platform	Control	Affected
GSE62232	Liver	HCV-related HCC	GPL570	10	12
GSE69715	Liver	HCV-related HCC	GPL570	66	37
GSE107170	Liver	HCV-related HCC	GPL570	31	44

(Dallakyan and Olson, 2015) to calculate binding energies of ligand molecules with target proteins. Autodock vina utilized an empirical scoring function to determine the affinity of protein-compound binding, which was calculated by aggregating contributions from various individual terms. The docked complex with the lowest root mean square deviation (RMSD), was considered the

Table 2
Selected active compound, their Oral Bioavailiability(OB), Drug-Likeness (DL), Molecular weight (MW), and PubChem IDs.

Plant Source	Active compounds	Oral Bioavailability (OB > 0.30)	Drug Likeness (DL > 0.18)	Molecular Weight (g/mol)	PubChem ID
Withania somnifera	(+)-Catechin	0.55	0.64	290.27	9064
	24-Methyldesmosterol	0.55	0.76	398.66	193,567
	Beta-Sitosterol	0.55	0.78	414.7	222,284
	Campesterol	0.55	0.59	400.7	173,183
	Fucosterol	0.55	0.85	412.7	5,281,328
	Kaempferol	0.55	0.5	286.24	5,280,863
	Oleanolic acid	0.85	0.37	456.7	10,494
	Quercetin	0.55	0.52	302.23	5,280,343
	Stigmasterol	0.55	0.62	412.7	5,280,794
	Stigmasterone	0.55	0.5	410.7	14,807,783
	Withaferin A	0.55	0.37	470.6	265,237
	Withanolide J	0.55	0.46	470.6	21,679,022
	Withanone	0.55	0.45	470.6	21,679,027
Senna alexandrina	Rhein	0.56	0.46	284.22	10,168
	Kaempferol	0.55	0.5	286.24	5,280,863
	Emodin-8-glucoside	0.55	0.74	432.4	99,649
	Rheinanthrone	0.56	0.89	270.24	119,396
	Aloe-emodin-8-O-beta-D-glucopyranoside	0.55	0.46	432.4	5,317,644
	Isorhamnetin	0.55	0.39	316.26	5,281,654
	Physcionin	0.55	0.19	446.4	4,484,071
	Tinnevellin glucoside	0.55	0.47	408.4	157,631
	Beta-Sitosterol	0.55	0.78	414.7	222,284
Rumex vesicarius	Retinol	0.55	0.73	286.5	445,354
	d-Tartaric acid	0.56	0.59	150.09	439,655
	Ascorbic acid	0.56	0.74	176.12	54,670,067
	Beta-Tocopherol	0.55	0.47	416.7	6,857,447
Rhazya stricta	Isovallesiachotamine	0.55	0.24	350.4	6,442,678
	2H-3,7-Methanoazacycloundecino(5,4-b)indole-9-carboxylic acid, 7-ethyl-1,4,5,6,7,8,9,10-octahydro-, methyl ester, (7S-(7R*,9S*))-	0.55	0.64	340.5	12,444,819
	Strictanol	0.55	0.38	298.4	12,314,913
	Tetrahydroalstonine	0.55	0.47	352.4	72,340
	Rhazimol	0.55	1.22	338.4	101,986,486
	Corynan-16-carboxylic acid, 16,17,19,20-tetradehydro-17-hydroxy-, methyl ester, (16E,19E)-	0.55	0.28	352.4	439,666
	Rhazinilam	0.55	0.44	294.4	11,312,435
	Rhazimal	0.55	0.73	350.4	101,967,159
	Quebrachamine	0.55	0.47	382.4	92,990
	Stemmadenine	0.55	0.67	354.4	443,367
	Methyl (10S,12R,13E,18S)-13-ethylidene-8,15-diazapentacyclo [10.5.1.01,9.02,7.010,15]octadeca-2,4,6,8-tetraene-18-carboxylate	0.55	1.04	322.4	6,444,325
	Ursolic acid	0.85	0.66	456.7	64,945
	Rhazimine	0.55	1.24	350.4	6,443,646
	15beta-Hydroxyvincadifformine	0.55	0.95	354.4	11,530,478
	(+)-Condylocarpine	0.55	0.9	322.4	10,914,255
	Vallesiachotamine	0.55	0.24	350.4	5,384,527
	Corynan-17-ol	0.55	0.31	298.4	164,952
	10-Hydroxyakuammicine	0.55	1.19	338.4	6,436,282
Pulicaria incisa	5-*O*-caffeoylquinic acid	0.11	0.79	354.31	5,280,633
	3, 5-di-*O*-caffeoylquinic acid	0.11	0.85	360.6	21,769,778
Heliotropium arbainense	12-Hydroxy-3-keto-bisnor-4-cholenic acid	0.85	0.95	360.5	536,316
	Lasiocarpine	0.55	0.18	411.5	5,281,735
Commicarpus grandiflorus	12-Hydroxy-3-keto-bisnor-4-cholenic acid	0.85	0.95	360.5	536,316
	Beta-Sitosterol	0.55	0.78	414.7	222,284
	Betulinic acid	0.85	0.25	456.7	64,971
Asphodelus fistulosu	Quercetin	0.55	0.52	302.23	5,280,343
	Beta-Sitosterol	0.55	0.78	414.7	222,284

optimal complex, and the binding energies among ligand and target protein were evaluated based on their affinity. A good binding strength was indicated by a value < -5.00 kcal/mol, while value < − 7.00 kcal/mol indicated very good affinity. Finally, visualization of docked complexes was performed using Discovery Studio (Studio, 2008), PyMOL (Yuan et al., 2017), and ChimeraX (Goddard et al., 2018) programs.

2.7. Molecular dynamic (MD) simulation

All-atom MD simulation is a computational method that employs explicit representation of every atom and bond in a system, allowing for a highly detailed examination of molecular dynamics. This technique involves solving the equations of motion for each atom in the system, based on the interatomic potentials that describe the interactions between them. This study utilized GROMACS 2018 software and the OPLS-AA/L force field to conduct MD simulations of docked complexes. The initial structures for the simulations were taken from 3D structure of the protein, and further optimization was done using the DockPrep tool (Pettersen et al., 2004). The MD simulation was initiated using docked complexes of ligand molecules with the target protein, which possessed the highest binding affinity, as the initial position. While the ligand molecule was parameterized through the SwissParam webserver (Zoete et al., 2011). Later, the MD simulations were carried out for 20 ns, following a previous studies (Alamri, 2020). General MD simulation parameters, particularly radius of gyration, RMSD, and Root mean square fluctuation (RMSF) (Needle et al., 2015) were evaluated for each complex.

3. Results

3.1. Identification of bioactive components

After searching and filtering, 53 compounds were obtained from *Withania somnifera,* 9 compounds from *Senna alexandrina,* 4 compounds from *Rumex vesicarius,* 18 compounds from *Rhazya stricta,* 2 compounds from *Pulicaria incisa,* 2 compounds from *Heliotropium arbainense,* 3 compounds from *Commicarpus grandifloras,* and 2 compounds from *Asphodelus fistulosus.* The duplicated compounds were removed, and a total of 48 compounds were selected as the putative components of 8 indigenous plants of Median valley. All these 48 compounds met the precise criteria of DL $\geq$ 0.18, OB $\geq$ 0.30, and molecular weight < 500 g/mol (Table 2).

The selected compounds were then evaluated for the ADME analysis. A total of 18 compounds namely (+)-Catechin, 24-Methyldesmosterol, Beta-Sitosterol, Campesterol, Fucosterol, Stigmasterol, Stigmasterone, Withanolide J, Kaempferol, Rheinanthrone, Isorhamnetin, d-Tartaric acid, Ascorbic acid, Beta-Tocopherol, Rhazimol, 5-O-caffeoylquinic acid, 3, 5-di-O-caffeoylquinic acid, and 12-Hydroxy-3-keto-bisnor-4-cholenic acid were found to have non-toxic effect with minimal BBB permeant and high GI absorption (Table 3). In ADMET analysis, hepatotoxicity refers to the potential for active compounds to cause damage to the liver, which can result in liver dysfunction or failure. In the current study, it is worth noting that all select compound has inactive hepatotoxicity. On the other hand, carcinogenicity refers to the potential for selected compounds to cause cancer, while mutagenicity indicates the ability of compounds to cause changes in DNA that may lead to genetic mutations, which can result in developmental abnormalities, cancer, or other diseases. If we compare with our findings, all selected compounds have inactive mutagenicity and carcinogenicity. To sum up, these results strengthened the findings of the current study that the indigenous plants of

Table 3
ADMET profiling of active compounds.

Compound	GI absorption	BBB permeant	P-gp substrate	CYP1A2 inhibitor	CYP2C19 inhibitor	CYP2C9 inhibitor	CYP2D6 inhibitor	CYP3A4 inhibitor	Log K_p (cm/s)	Hepatotoxicity	Carcinogenicity	Mutagenicity	Cytotoxicity
(+)-Catechin	High	×	✓	×	×	×	×	×	−7.82	×	×	×	×
24-Methyldesmosterol	Low	×	×	×	×	✓	×	×	−2.55	×	×	×	×
Beta-Sitosterol	Low	×	×	×	×	×	×	×	−2.20	×	×	×	×
Campesterol	Low	×	×	×	×	×	×	×	−2.50	×	×	×	×
Fucosterol	Low	×	×	×	×	×	×	×	−2.53	×	×	×	×
Stigmasterol	Low	×	×	×	×	✓	×	×	−2.74	×	×	×	×
Stigmasterone	Low	×	×	×	×	✓	×	×	−2.98	×	×	×	×
Withanolide J	High	×	✓	×	×	×	×	×	−7.46	×	×	×	×
Kaempferol	High	×	×	✓	×	×	×	×	−6.70	×	×	×	×
Rheinanthrone	High	×	×	×	×	×	×	×	−6.02	×	×	×	×
Isorhamnetin	High	×	×	✓	×	×	×	×	−6.90	×	×	×	×
d-Tartaric acid	Low	×	×	×	×	×	×	×	−8.55	×	×	×	×
Ascorbic acid	High	×	×	×	×	×	×	×	−8.54	×	×	×	×
Beta-Tocopherol	Low	×	✓	×	×	×	×	×	−1.51	×	×	×	×
Rhazimol	High	×	×	×	×	×	×	×	−9.59	×	×	×	×
5-O-caffeoylquinic acid	Low	×	×	×	×	×	×	×	−8.76	×	×	×	×
3, 5-di-O-caffeoylquinic acid	Low	×	✓	✓	×	×	×	×	−9.55	×	×	×	×
12-Hydroxy-3-keto-bisnor-4-cholenic acid	High	×	✓	×	×	×	×	×	−6.28	×	×	×	×

Medina valley have drug-like active compounds which might have a key role to play in the prevention and disease.

3.2. 2.2. Known therapeutic targets acting on HCV-related HCC

Three microarray datasets including GSE62232, GSE69715, and GSE107170 were retrieved from the NCBI-GEO database and were further processed using Limma package of R for the identification of DEGs. In the Limma package, the p-value and LogFC criteria were set as LogFC > 1.0 and p-value < 0.05 for screening of DEGs. A total of 2484 DEGs (1089 upregulated and 1395 downregulated) DEGs obtained from GSE62232 datasets, 2091 DEGs (533 upregulated and 1558 downregulated) from GSE69715, and 1618 DEGs (384 downregulated and 1234 upregulated) from GSE107170 (Fig. 1). The final DEGs were then used as known therapeutic targets of HCV-related HCC.

3.3. Compound-target network construction

After disease-related target prediction, a venn diagram was plotted for the identification of overlapped genes between plant-related targets and disease-related targets. Further, 1592 potential target genes of 18 compounds were collected from the Swiss Target Prediction and STITCH database. The Venn diagram unveiled 139 potential anti-HCV-related HCC genes of 8 indigenous plants of Medina valley which were later considered for further analysis. The compound along with their corresponding targets was imported to Cytoscape for visualization of the hub compound within the network. The compound-target network demonstrated that predicted targets may simultaneously induce a synergistic effect when these medicinal plants serve as an anti-cancer agent.

3.4. Functional annotation of overlapped targets

GO and pathway enrichment analysis of overlapped proteins were conducted using DAVID resources for the identification of their biological characteristics. There were respectively 186 BP, 41 CC, and 69 MF terms in total, which fulfill the criteria of p-value<0.05. The top 20 GO terms indicated that overlapped genes may regulate cancer cell proliferation via regulation of T cell apoptotic process, inflammatory response, positive regulation of protein kinase B signaling, identical protein binding, enzyme binding, extracellular exosome, cytosol, plasma membrane, endoplasmic reticulum, and macromolecular complex. To explore the underlying involved pathways of overlapped targets in HCV-related hepatocellular carcinoma, KEGG pathway analysis of overlapped genes was conducted. More importantly, the majority of common genes exhibited pathways in cancer (21 counts). KEGG pathway analysis uncovered that the genes were concentrated in metabolic pathways, p53 signaling pathway, chemical carcinogenesis, PI3K-Akt signaling pathway, ovarian steroidogenesis, and endocrine resistance. The bubble map of top signification terms and pathways was shown in Fig. 2.

3.5. Identification of hub genes

The PPI network of overlapped targets was constructed through STRING database. This network consists of 133 nodes and 626 edges. From these 133 nodes, the top 10 nodes based on their

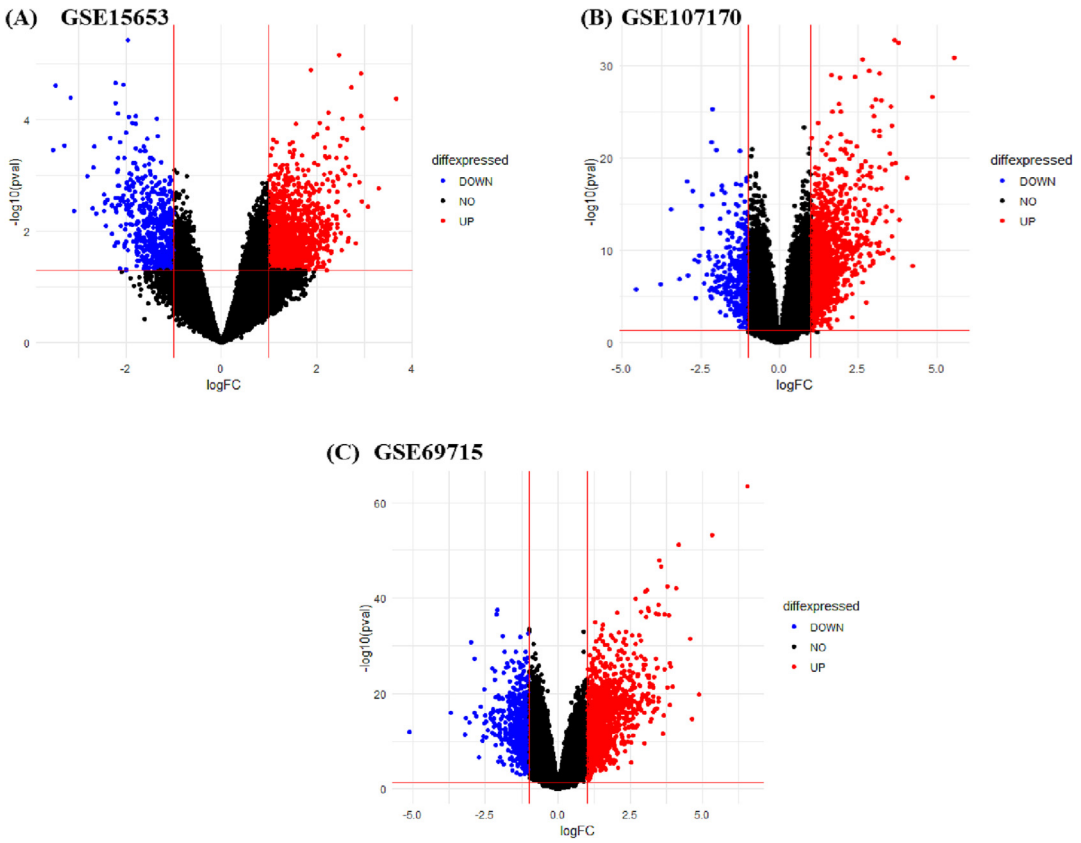

Fig. 1. Pictorial representation of DEGs through Volcano plot with red and blue dots indicating the upregulated and downregulated genes respectively. While non-significant genes are represented using grey color.

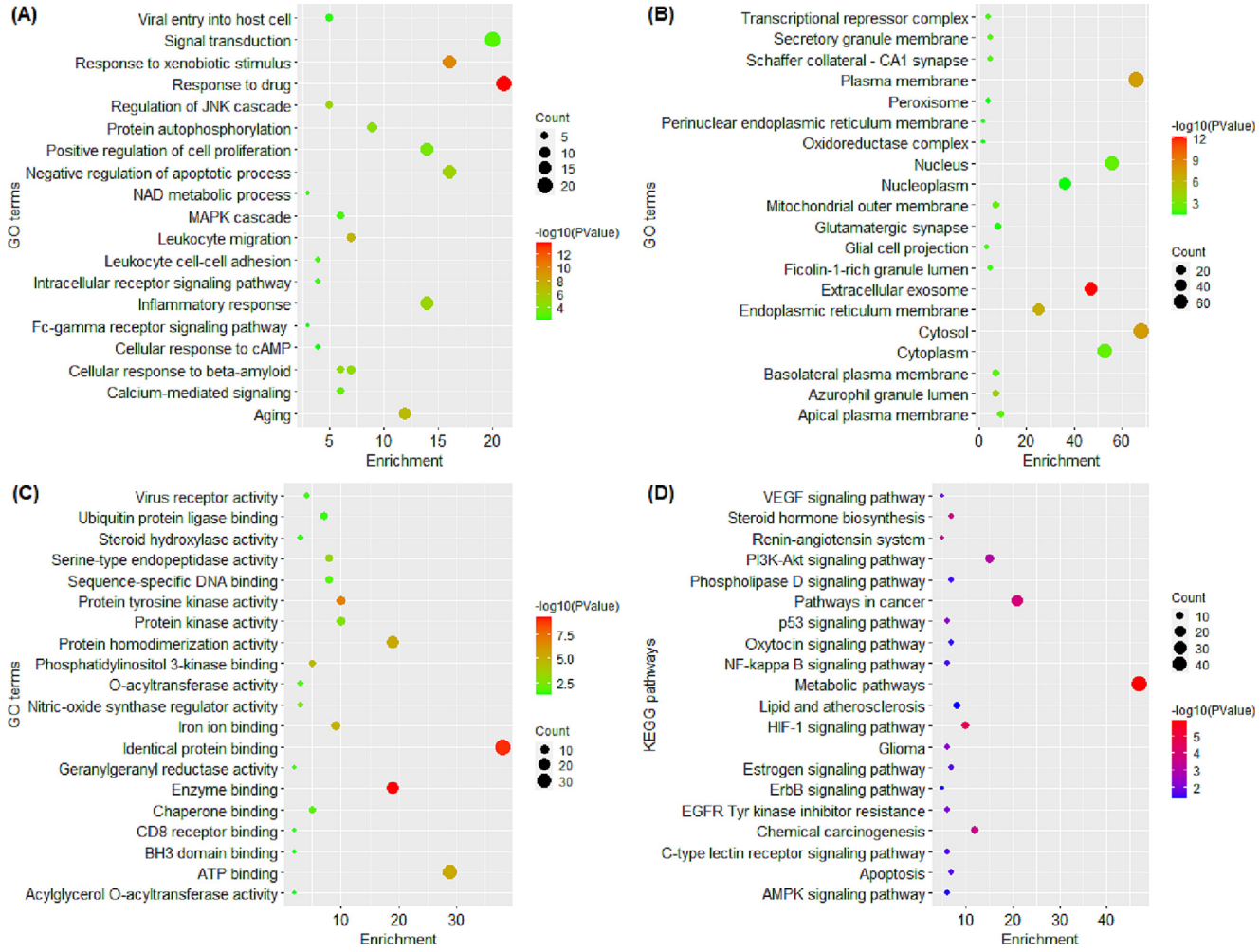

Fig. 2. Bubble plot representing Gene ontology with respect to **(A)** biological processes, **(B)** cellular components, **(C)** molecular functions, **(D)** and KEGG pathways.

degree of connectivity were selected as the hub genes. These hub genes are ALB (61), EGFR (42), *ESR1* (41), JUN (36), MMP9 (31), PTGS2 (28), AR (28), MDM2 (24), CDK1 (21), and CYP3A4 (20) (Fig. 3). These nodes may play a pivotal role in the PPI network for the anti-cancer effect. The compound and target information on the top 10 nodes are listed in Table 4, where the closeness centrality is the center proximity, radiality is the radial degree, and betweenness centrality indicates the nodes that play bridge spanning roles in network.

3.6. Compound-Target-Disease network

To develop a more intuitive comprehension of the mechanisms responsible for the impact effect on indigenous plants in HCV-related HCC, an integrated "compound-target-disease" network was generated based on the GO and the KEGG route map (Fig. 4). Pathway that are not directly associated with the HCV-related HCC were removed. Through systematic analysis of the compound-target network, PPI network, and compound-target-disease network, top ranked proteins including ALB and PTGS2 were selected for molecular docking. ALB and PTGS2 have higher degree of connectivity within PPI network as well as the majority of the compounds were found to be targeted by these hub genes. Secondly, GO term analysis revealed that genes may regulate the cancer cell proliferation through identical protein binding, and negative regulation of apoptotic process while the KEGG pathway uncovered that PTGS2 is enriched in pathways including chemical carcinogenesis, metabolic pathways, pathways in cancer, etc.

3.7. Molecular docking analysis

Through PPI network analysis and target screening, two proteins named ALB and PTGS2 were used for molecular docking analysis. The selected 18 compounds were then docked against ALB and PTGS2 in order to predict their binding affinity and stability, and free energy with the active site of the target protein (Williams-Noonan et al., 2018, Guedes et al., 2014). Currently, the approximation of binding free energy is an important objective of docking protocols, which is revealed in terms of hydrogen bonds, total internal energy, the energy of dispersion and repulsion, torsional free energy, electrostatic force, the energy of desolvation, and unbound system's energy (Luo et al., 2022). The top compounds, having the highest binding energy (<-5.00 kcal/mol) were selected for further analysis. In the case of ALB protein, kaempferol (-5.2 kcal/mol), rhazimol (-5.9 kcal/mol), beta-sitosterol (-6.2 kcal/mol), 12-Hydroxy-3-keto-bisnor-4-cholenic_acid (-7.0 kcal/mol), and 5-O-caffeoylquinic_acid (-6.0 kcal/mol) has highest binding affinity as compared to other active compounds (Fig. 5). In case of ALB-5-O-caffeoylquinic_acid complex binding affinity was contributed the hydrogen bonding with the Ser B:27, Ser B:72, Glu B:23, Gly B:25, and His B:71 residues. In terms of 12-Hydroxy-3-keto-bisnor-4-cholenic_acid, ALB has hydrogen bonding interac-

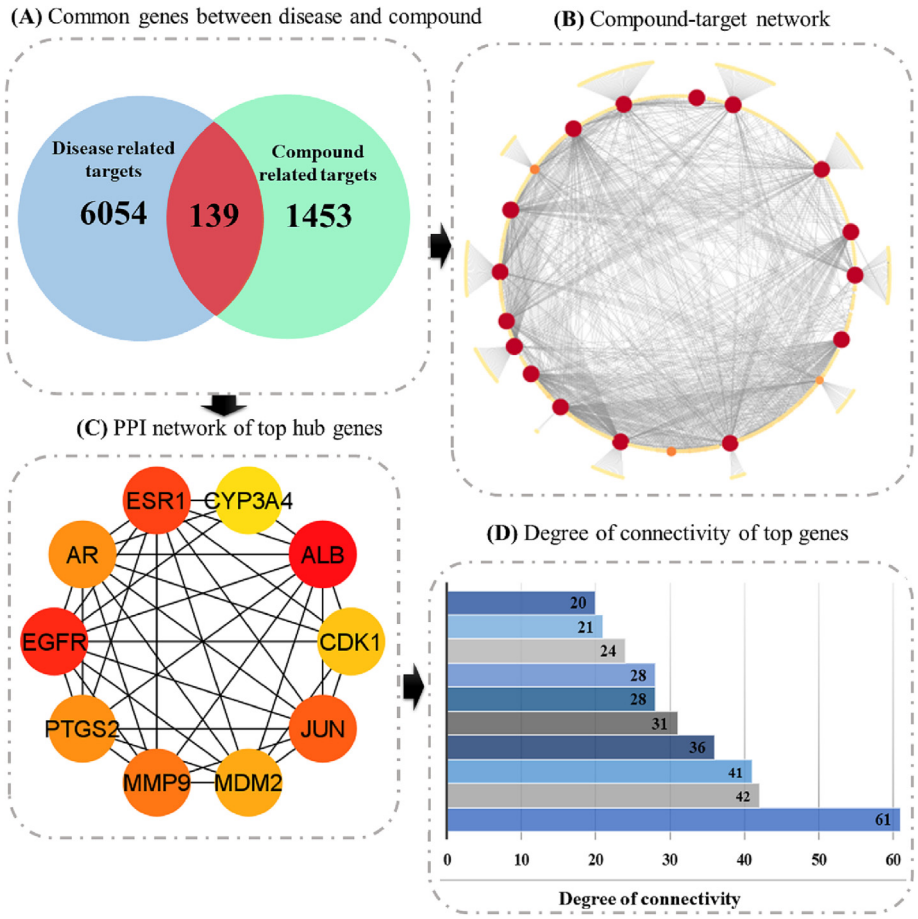

Fig. 3. **(A)** Venn plot of common genes among plants and disease, **(B)** Compound-target network, where the size indicates their degree of connectivity, **(C)** Top 10 genes ranked based on degree algorithm, **(D)** Bar plot representing the degree of each hub gene.

Table 4
Interaction network data of top 10 hub genes.

Sr.No.	Name	Degree	Closeness	Betweenness	Radiality
1	ALB	61	94.33333	5559.591	7.424242
2	EGFR	42	82.83333	1859.256	7.174242
3	ESR1	41	82.45	1743.784	7.166667
4	JUN	36	80	1014.448	7.143939
5	MMP9	31	75.28333	521.8788	6.984848
6	PTGS2	28	75.11667	729.5465	7.030303
7	AR	28	75.11667	646.2724	7.022727
8	MDM2	24	72.2	668.1914	6.954545
9	CDK1	21	70.66667	468.2167	6.939394
10	CYP3A4	20	70.86667	602.4295	6.962121

tion with Gly B:69, Gly B:25, His B:71, Ile B:24, and Glu B:77; for beta-sitosterol, ALB demonstrating hydrogen bond interaction with Glu A:13, Glu B:77, Leu A: 12, and Leu A:6; for kaempferol, the hydrogen bonding interaction was found to be Ile B: 24, Glu B:23, Phe A:7, and the rhazimol showed hydrogen binding interaction with His B:71, Ser B:72, and Glu B:77 residues (Table 5).

In the case of PTGS2 protein, 24-Methyldesmosterol (-8.4 kcal/mol), beta-sitosterol (-8.3 kcal/mol), stigmasterone (-8.0 kcal/mol), fucosterol (-8.7 kcal/mol), and Withanolide_J (-9.5 kcal/mol)has highest binding affinity in comparison with other active compounds (Fig. 6). In the case of PTGS2- 24-Methyldesmosterol complex binding affinity contributed the hydrogen bonding with the Val A:444, His A: 388, Leu A: 294, Gln A:203; for beta-sitosterol PTGS2 has hydrogen bonding interaction with Ile A: 408, His A: 388, Tyr A: 385, Leu A: 294; for fucosterol, PTGS2 demonstrating Ile A: 408, Tyr A: 385, Leu A: 294, Gln A:203; for stigmasterone, hydrogen bonding interaction were found to be His A: 388, Leu A: 294, Ile A: 408, Tyr A: 385; and Withanolide_J showed hydrogen binding interaction with Val A:447, His A: 388, Leu A: 390, Ala A:202 residues (Table 6).

3.8. MD simulation

To evaluate the association of ALB and PTGS2 protein and for evaluating the stability of the ligand molecules, all-atom MD simulations were performed for 20 ns using GROMACS. The top two complexes from each protein were selected for MD simulation for measuring their RMSD and RMSF values which ultimately

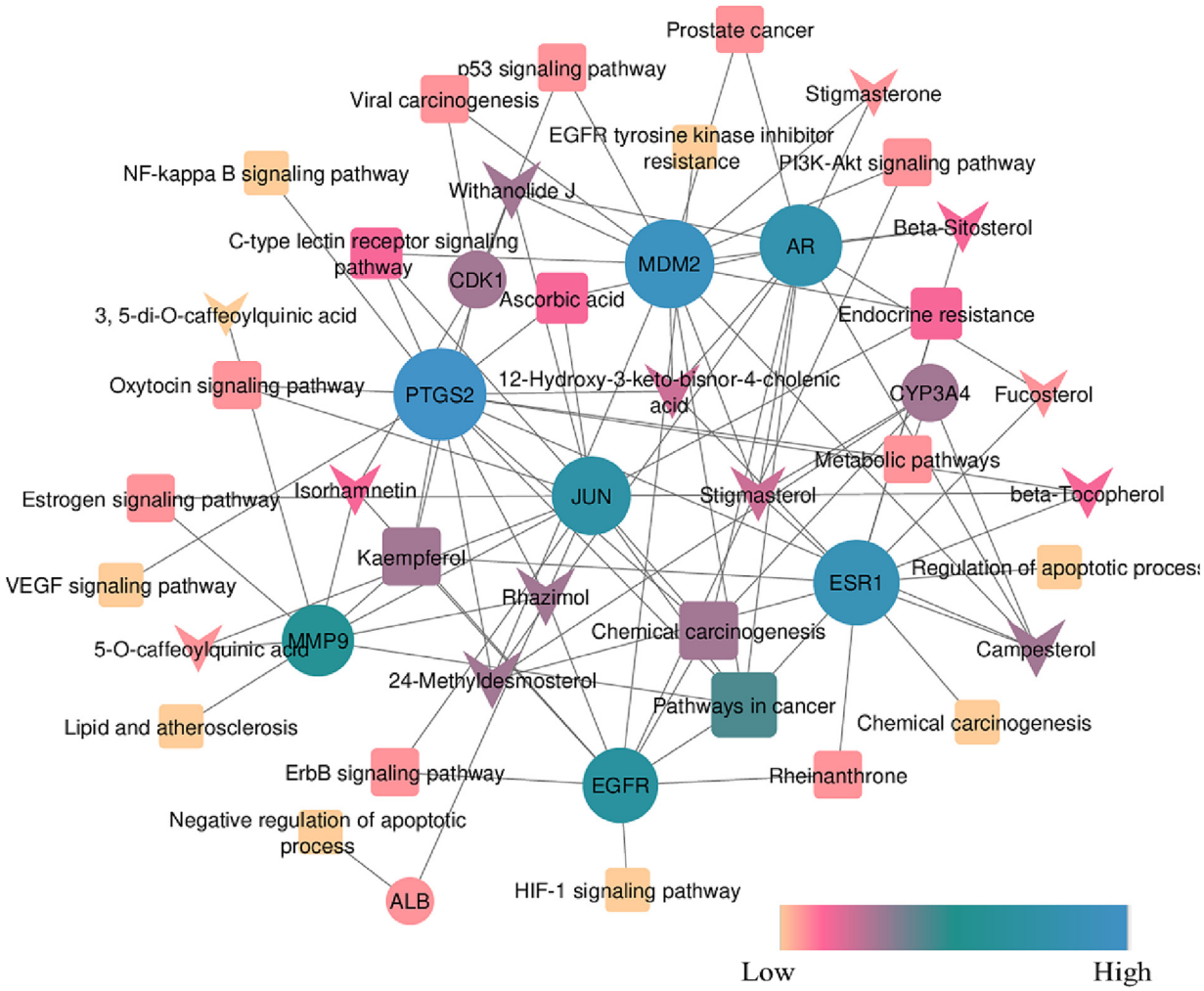

Fig. 4. Compound-Target-Disease network. The size of nodes indicates their degree of connectivity. The circle represents hub proteins, the square represents targeted pathways, while arrows represent the active compounds.

helped in determining the stability of the docked complex. RMSD measures the deviation of the docked complex from its initial structure over the course of the simulation, while RMSF measures the deviation of each atom in the complex from its average position. Both measures are used to evaluate the stability and flexibility of the complex during the simulation period, and can be used to identify the most stable and flexible regions of the complex. The RMSD analysis indicated that the majority of complexes reached equilibrium within 20 ns, indicating high stability of docked complexes. However, some fluctuations were observed within the first 10 ns in all systems. The RMSD values for the ALB complex with 5-O-caffeoylquinic_acid and 12-Hydroxy-3-keto-bisnor-4-cholenic_acid stabilized around ~ 0.3 nm and 0.12 nm respectively (Fig. 7**(A)**), while those for the PTGS2 complex with beta-sitosterol and withanolide_J were equilibrated at around ~ 0.18 nm (Fig. 8**(A)**). These findings suggested that the binding of 5-O-caffeoylquinic_acid and 12-Hydroxy-3-keto-bisnor-4-cholenic_acid to ALB could cause conformational changes. This was further supported by the analysis of RMSF vs ALB residue number, which indicated that the 5-O-caffeoylquinic_acid and 12-Hydroxy-3-keto-bisnor-4-cholenic_acid complexes showed higher oscillations in backbone residues (Fig. 7**(B)**) compared to the PTGS2 complex with beta-sitosterol and withanolide_J (Fig. 8**(B)**).

The radius of gyration (Rg) is a crucial parameter to evaluate changes in the compactness of a ligand–protein complex. In the case of ALB, 12-Hydroxy-3-keto-bisnor-4-cholenic_acid and 5-O-caffeoylquinic_acid complexes demonstrated constant compactness throughout the simulation, as evidenced by the constant Rg values (Fig. 7**(C)**). In the case of PTGS2, withanolide_J showed high fluctuations as compared to beta-sitosterol, which was in agreement with its lowest binding free energy predicted through docking studies (Fig. 8**(C)**). Furthermore, the findings obtained from the analysis of RMSD, RMSF, and Rg parameters suggested that all the complexes remained stable throughout the simulation period. Thus, it can be inferred that these compounds are potential candidates for inhibiting ALB and PTGS2, which should be further validated through *in vivo* and *in vitro* studies.

4. Discussion

The prevalence of HCV-associated HCC in Saudi Arabia is relatively high compared to other countries and is therefore considered as a significant public health issue within the country (Thrift et al., 2017, Alavian and Haghbin, 2016). A recent study indicated that HCV was found to be the major causative agent of HCC in Saudi Arabia, accounting for 59% of all cases (Althubiti and Alfayez, 2021). Their study provides shreds of evidence that the prevalence of HCV infection in patients with HCC was significantly higher in Saudi Arabia compared to other regions, such as Egypt and Iran. Several factors contribute to the extreme preva-

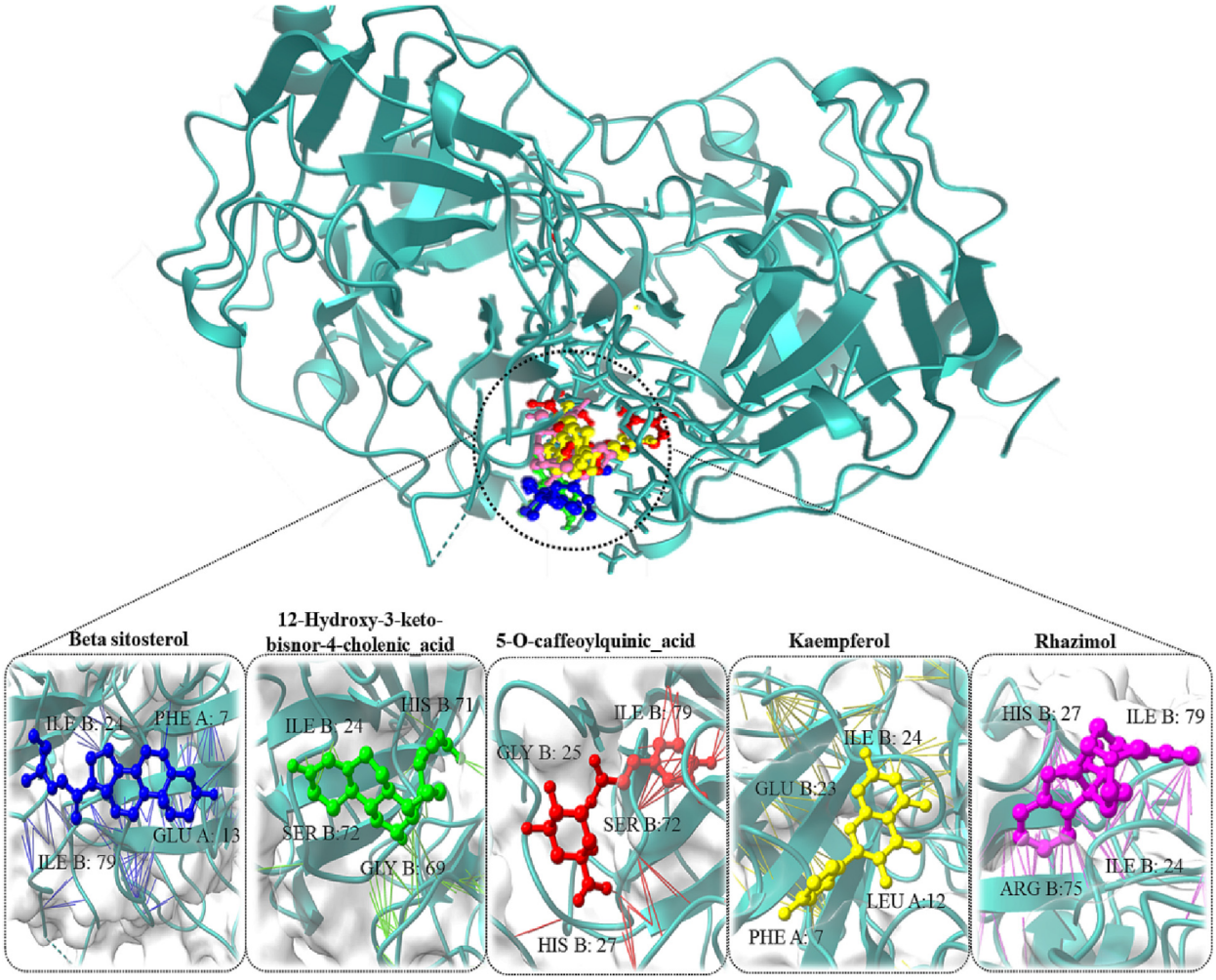

Fig. 5. The docked complexes of ALB protein along with their strongest binding compounds.

Table 5
Binding energy and interactions of active compounds with ALB protein.

Protein-ligand complex	Binding Affinity (kcal/mol)	RMSD	Interacting residues
IKTS_Kaempferol	−5	2.702	Ile B: 24, Glu B:23, Phe A:7
IKTS_Rhazimol	−5.9	1.095	His B:71, Ser B:72, Glu B:77
IKTS_Beta-Sitosterol	−6.2	3.208	Glu A:13, Glu B:77, Leu A: 12, Leu A:6
IKTS_12-Hydroxy-3-keto-bisnor-4-cholenic_acid	−7	0.972	Gly B:69, Gly B:25, His B:71, ILE B:24, Glu B:77
IKTS_5-O-caffeoylquinic_acid	−6	2.994	Ser B:27, Ser B:72, Glu B:23, Gly B:25, His B:71

lence of HCV-associated HCC in Saudi Arabia, including the widespread use of contaminated needles in medical procedures, high rates of blood transfusions, and poor infection control measures in healthcare settings (Ashtari et al., 2015). In recent years, the Saudi Arabian government has implemented several initiatives to combat HCV and HCC, including the introduction of vaccination programs and the establishment of specialized clinics for the management of HCV-related HCC. Overall, the high prevalence of HCV-associated HCC in Saudi Arabia highlights the need for continued efforts to improve infection control measures and increase public awareness about the risks of HCV infection.

In the present work, the network pharmacology approach was used for the systems-level view of the molecular interactions underlying HCV-related HCC, which lends a helping hand in the identification of new therapeutic strategies for improving patient outcomes. At first, the information related to active constituents of indigenous plants was collected from publically available repositories and published literature. The anti-cancer activity of 8 plants namely *Rumex vesicarius, Withania somnifera, Rhazya stricta, Heliotropium arbainense, Asphodelus fistulosus, Pulicaria incise, Commicarpus grandiflorus,* and *Senna alexandrina,* were studied. These are the local plants of Medina valley and have the potential to be used as medicine to provide benefits to humanity. After the screening of active compounds, the disease-related data of HCV-related HCC were collected from microarray datasets. For this, Limma package was run on the selected microarray datasets for the identification of DEGs which were later compared with target genes of plant-related compounds. The overlapped genes obtained after comparison were subjected to network pharmacology approach for analyzing the multi-target effect of screened active compounds against HCV-related HCC proteins. The pathway enrichment analysis uncovered that overlapped genes are mainly involved in HIF-1

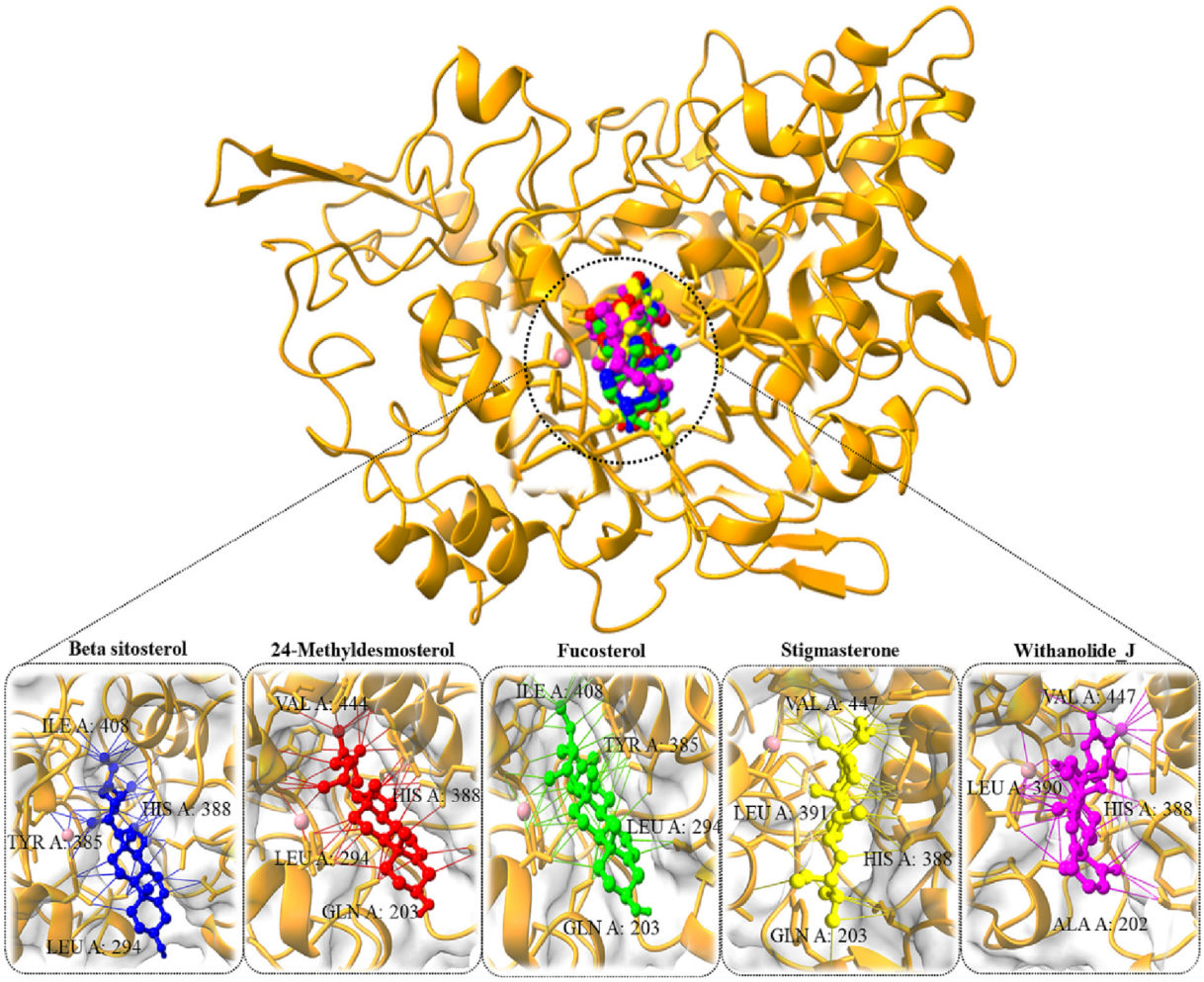

Fig. 6. The docked complexes of PTGS2 protein along with their strongest binding compounds.

Table 6
Binding energy and interactions of active compounds with PTGS2 protein.

Protein-ligand complex	Binding Affinity (kcal/mol)	RMSD	Interacting residues
5IKQ_24-Methyldesmosterol	−8.4	0.776	Val A:444, His A: 388, Leu A: 294, Gln A:203
5IKQ_Beta-Sitosterol	−8.3	2.182	Ile A: 408, His A: 388, Tyr A: 385, Leu A: 294
5IKQ_Stigmasterone	−8	2.072	His A: 388, Leu A: 294, Ile A: 408, Tyr A: 385
5IKQ_Fucosterol	−8.7	1.408	Ile A: 408, Tyr A: 385, Leu A: 294, Gln A:203
5IKQ_Withanolide_J	−9.5	2.527	Val A:447, His A: 388, Leu A: 390, Ala A:202

signaling pathway, pathways in cancer, PI3K-Akt signaling pathway, ErbB signaling pathway, C-type lectin receptor signaling pathway, and oxytocin signaling pathway.

In HCV-related HCC, the PI3K-Akt signaling pathway is often dysregulated, contributing to the development and progression of HCC (Irshad et al., 2017). The virus activates the PI3K-Akt pathway through several mechanisms, including the activation of growth factor receptors including IGF-1R, EGFR, and c-Met (Józefiak et al., 2021, Mahmoudvand et al., 2019, Arzumanyan et al., 2013). HCV also activates PI3K-Akt signaling and promotes HCC cell survival and growth by stimulating protein synthesis, inhibiting apoptosis, and enhancing cell proliferation (Paskeh et al., 2022). Moreover, activation of PI3K-Akt pathway has been associated with the development of drug resistance in HCC (Feng et al., 2020, Zou et al., 2020). Thus, by targeting the genes involved in PI3K-Akt pathways, the progression of HCC can be reduced significantly.

In HCV-related HCC, studies reported that C-type lectin receptor (CLR) plays a significant role in regulating the immune response against HCV infection, as well as in the development of chronic inflammation, which contributes to the proliferation of HCC (Cabral et al., 2022, Boltjes et al., 2014). Moreover, the production of cytokines and chemokines in response to virus infection can contribute to the recruitment of inflammatory cells, such as macrophages, into the liver, which promotes the development of cirrhosis in affected individuals (Al-Qahtani et al., 2014). Therefore, targeting the CLR signaling pathway may be a promising approach for treating HCV-related HCC. For example, blocking the activation of CLRs or the downstream signaling pathways may help to reduce inflammation and prevent the development and progression of HCC.

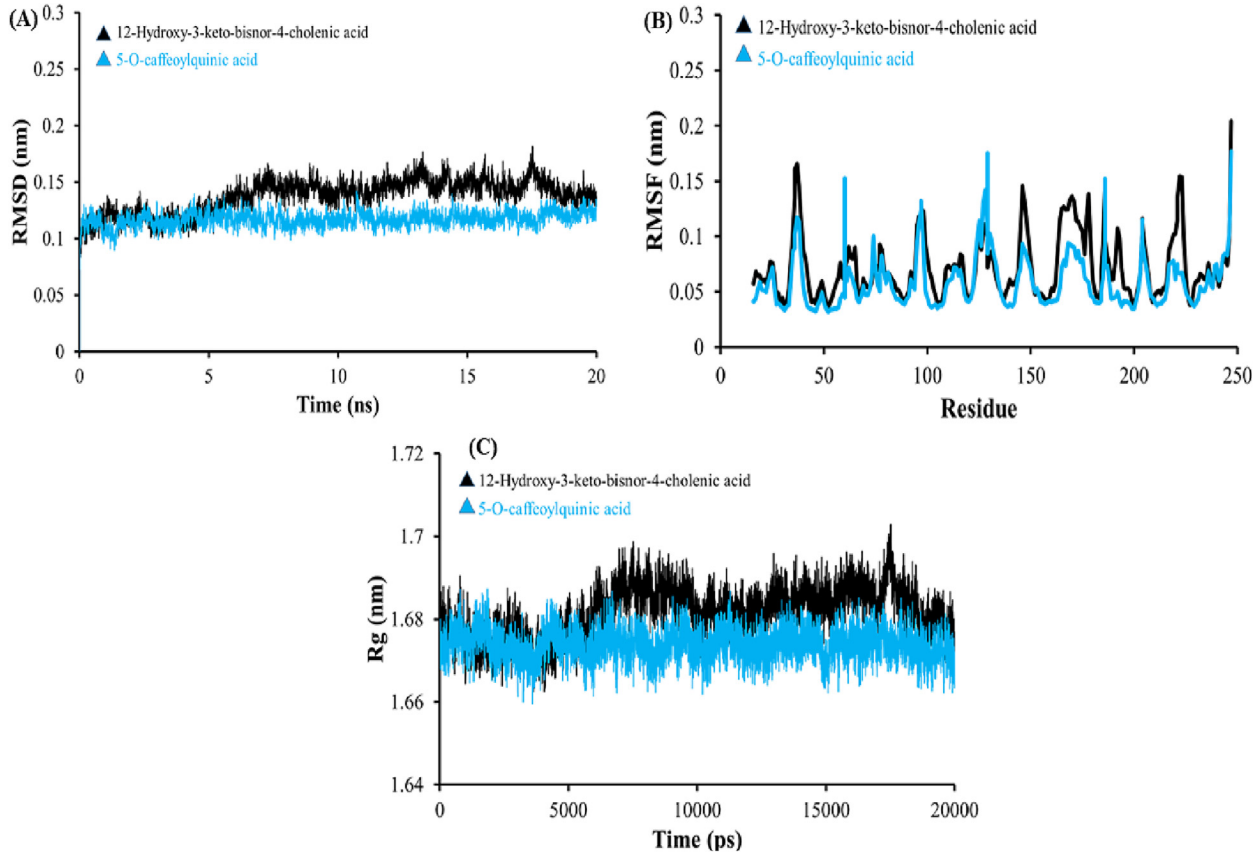

Fig. 7. **(A)** RMSD of backbone atoms (C, Cα, and N) for ALB-Ligand complex systems. **(B)** RMSF of backbone atoms for ALB-Ligand complex systems. **(C)** Rg of backbone atoms.

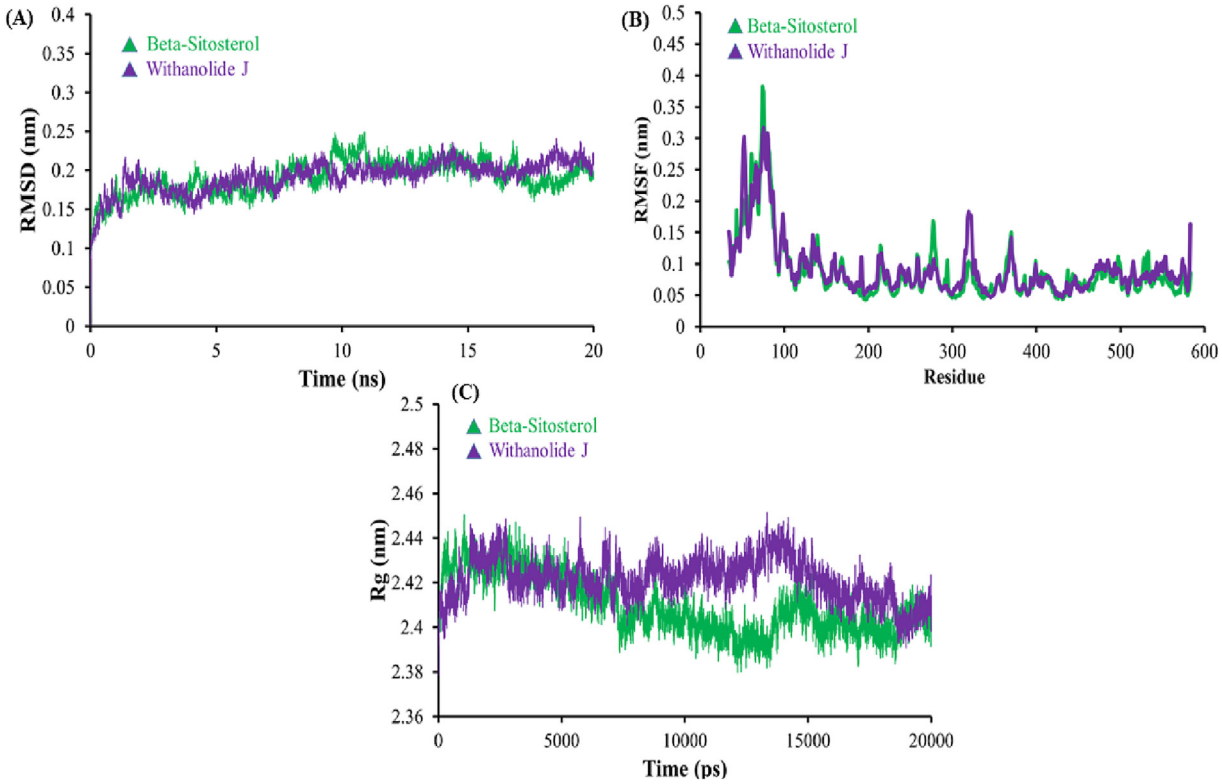

Fig. 8. **(A)** RMSD of backbone atoms (C, Cα, and N) for PTGS2-Ligand complex systems. **(B)** RMSF of backbone atoms for PTGS2-Ligand complex systems. **(C)** Rg of backbone atoms.

After pathway enrichment analysis, two proteins namely ALB and PTGS2 were selected as the hub proteins as these proteins have a higher degree of connectivity within the compound-target network and compound-target-disease network. Later, docking analysis were performed to analyze the interaction of ALB and PTGS2 with screened compounds of local plants of Medina valley. Molecular docking, however, only offers information for estimating compound suitability at a protein active site. As a result, the use of MD simulation and derived binding energy values to evaluate compound to protein target systems has increased the dependence on binding conformation data. MD simulation helps in analyzing the dynamics of docked complexes and the fluctuations in its energy landscape, providing insights into the stability of the complex and the potential for ligand-induced conformational changes in the protein. In short, molecular docking and dynamics simulation analysis unveiled significant binding affinity between active compound-protein matrices.

If we compare our findings with previous studies, then it is noteworthy that PTGS2 promotes of cell proliferation and survival in HCC by activating the MAPK and PI3K-Akt signaling pathways, which promote cell cycle progression and inhibit apoptosis (Zhang et al., 2022, Shi et al., 2022). In addition to its role in promoting HCC growth and progression, PTGS2 overexpression has been associated with resistance to chemotherapy and targeted therapies, including sorafenib (Nie et al., 2018, Ladd et al.). Thus, targeting PTGS2 with active compounds might be an effective therapeutic approach for treating HCC. On the other hand, the presence of inflammation, oxidative stress, and malnutrition in HCC can also contribute to the decreased level of ALB (Liu et al., 2020). The decreased level of ALB is often used as a biomarker for the severity of liver disease and the progression of HCC (Wang et al., 2013). Further, ALB suppresses the production of TNF-α and IL-6 cytokine which can promote the development and progression of HCC (Li et al., 2017). Moreover, ALB promotes the differentiation of T cells into regulatory T cells, which can suppress the proliferation of cancer cells and prevent their invasion and metastasis (Zhang et al., 2021). Overall, the role of ALB in HCC is complex and multifaceted, therefore, targeting ALB protein with active compounds can assists in developing effective therapeutic strategies based on ALB.

To sum up, our study provides a scientific foundation to unveil the multi-target effect of the indigenous plant of Medina valley as a promising treatment option for liver cancer. Thus, the integration of network pharmacology with bioinformatics approaches can help to identify the key molecular pathways and interactions that contribute to HCV-related HCC, and can be used to identify potential drug targets that can be modulated to treat this disease. Despite that, we validate our results through molecular docking as well as MD simulation, however additional *in vivo* and *in vitro* studies are required to validate the efficacy of current findings. There are several limitations to our study. First, additional tests are required to confirm our findings. Second, a larger database of traditional medicines and target genes is required, which improved the accuracy of the network pharmacology analysis results. Thirdly, even after combining the outcomes of network pharmacology with molecular docking, our study was unable to fully comprehend the precise therapeutic mechanism of local plants for treating HCV-related HCC. Thus, the integration of multiple disciplines was necessary to understand the action mechanism of these local plants in HCC.

5. Conclusion

The burden of HCV-related HCC in Saudi Arabia underscores the importance of effective strategies for the prevention, screening, and management of HCV infection and its complications. This high burden of HCV-related HCC in Saudi Arabia highlights the urgent need for the development of new and effective treatments for HCV infection and its associated complications. Regarding this, our study proposes a new scientific methodology for assessing the multi-component, multi-target effect of active compounds of local plants particularly those belonging to Medina valley. The current study integrated network pharmacology with bioinformatics approaches and proposed (+)-Catechin, 24-Methyldesmosterol, beta-sitosterol, campesterol, fucosterol, stigmasterol, stigmasterone, withanolide J, kaempferol, rheinanthrone, isorhamnetin, d-Tartaric acid, ascorbic acid, beta-tocopherol, rhazimol, 5-O-caffeoylquinic acid, 3, 5-di-O-caffeoylquinic acid, 12-Hydroxy-3-keto-bisnor-4-cholenic acid as the potential compounds for treating HCV-related HCC. Additionally, our findings highlighted that ALB and PTGS2 are potential therapeutic targets for reducing the incidence of cell growth and proliferation. In short, this study enriched our knowledge about the chemical composition of indigenous plants of Medina valley, as well as the synergistic mechanism of active compounds against HCV-related HCC.

Funding

The author extends his appreciation to Prince Sattam bin Abdulaziz University for funding this research work through the project number (PSAU/2022/01/23401).

Declaration of Competing Interest

The authors declare that they have no known competing financial interests or personal relationships that could have appeared to influence the work reported in this paper.

Acknowledgement

The author thanks the Deanship of Scientific Research (DSR), Prince Sattam bin Abdulaziz University, Al-Kharj, Saudi Arabia for providing the funding for this research.

References

Alamri, M.A., 2020. Pharmacoinformatics and molecular dynamic simulation studies to identify potential small-molecule inhibitors of WNK-SPAK/OSR1 signaling that mimic the RFQV motifs of WNK kinases. Arab. J. Chem 13, 5107–5117. https://doi.org/10.1016/j.arabjc.2020.02.010.

Alavian, S. M. & Haghbin, H. 2016. Relative importance of hepatitis B and C viruses in hepatocellular carcinoma in EMRO countries and the Middle East: a systematic review. Hepat. Mon. 16, e35106. https://doi.org/10.5812%2Fhepatmon.35106.

Al-Qahtani, A.A., Al-Anazi, M.R., Al-Zoghaibi, F., Abdo, A.A., Sanai, F.M., Khan, M.Q., Albenmousa, A., Al-Ashgar, H.I., Al-Ahdal, M.N., 2014. The association of toll-like receptor 4 polymorphism with hepatitis C virus infection in Saudi Arabian patients. BioMed Res. Int. 2014. https://doi.org/10.1155/2014/357062.

Alsaedi, S., Aljeddani, G., 2022. Phytochemical Analysis and Bioactivity Screening of Primary and Secondary Metabolic Products of Medicinal Plants in the Valleys of Medina Region Saudi Arabia. Adv. Biol. Chem. 12, 92–115. https://doi.org/10.4236/abc.2022.124009.

Althubiti, M. & Alfayez, M. 2021. Insights on Hepatocellular Carcinoma in Saudi Arabia. Liver Cancer in the Middle East. Ann. Romanian Soc. Cell Biol. 247-257.

Arzumanyan, A., Reis, H.M., Feitelson, M.A., 2013. Pathogenic mechanisms in HBV- and HCV-associated hepatocellular carcinoma. Nat. Rev. Cancer. 13, 123–135. https://doi.org/10.1038/nrc3449.

Ashtari, S., Pourhoseingholi, M.A., Sharifian, A., Zali, M.R., 2015. Hepatocellular carcinoma in Asia: Prevention strategy and planning. World J. Hepatol. 7, 1708 10.4254%2Fwjh.v7.i12.1708.

Banerjee, P., Eckert, A.O., Schrey, A.K., Preissner, R.J.N.A.R., 2018. ProTox-II: a webserver for the prediction of toxicity of chemicals. Nucleic Acids Res. 46, W257–W263. https://doi.org/10.1093/nar/gky318.

Boltjes, A., Movita, D., Boonstra, A., Woltman, A.M., 2014. The role of Kupffer cells in hepatitis B and hepatitis C virus infections. J. Hepatol. 61, 660–671. https://doi.org/10.1016/j.jhep.2014.04.026.

Cabral, L.K.D., Grisetti, L., Pratama, M.Y., Tiribelli, C., Pascut, D., 2022. Biomarkers for the Detection and Management of Hepatocellular Carcinoma in Patients Treated

with Direct-Acting Antivirals. Cancers 14, 2700. https://doi.org/10.3390/cancers14112700.
Chandran, U., Mehendale, N., Patil, S., Chaguturu, R., Patwardhan, B., 2017. Network pharmacology. Innov. Approaches Drug Dis. 127 10.1016%2FB978-0-12-801814-9.00005-2.
Clough, E., Barrett, T., 2016. The gene expression omnibus database. Methods Mol. Biol. https://doi.org/10.1007/978-1-4939-3578-9_5.
Daina, A., Michielin, O., Zoete, V., 2017. SwissADME: a free web tool to evaluate pharmacokinetics, drug-likeness and medicinal chemistry friendliness of small molecules. Sci. Rep. 7, 1–13. https://doi.org/10.1038/srep42717.
Dallakyan, S. & Olson, A. 2015. Small-molecule library screening by docking with PyRx. Chemical biology. Springer.
Dennis, G., Sherman, B.T., Hosack, D.A., Yang, J., Gao, W., Lane, H.C., Lempicki, R.A., 2003. DAVID: database for annotation, visualization, and integrated discovery. Genome Biol. 4, 1–11. https://doi.org/10.1186/gb-2003-4-9-r60.
Feng, J., Li, J., Wu, L., Yu, Q., Ji, J., Wu, J., Dai, W., Guo, C., 2020. Emerging roles and the regulation of aerobic glycolysis in hepatocellular carcinoma. J. Exp. Clin. Cancer Res. 39, 1–19. https://doi.org/10.1186/s13046-020-01629-4.
Gfeller, D., Grosdidier, A., Wirth, M., Daina, A., Michielin, O., Zoete, V., 2014. SwissTargetPrediction: a web server for target prediction of bioactive small molecules. Nucleic Acids Res. 42, W32–W38. https://doi.org/10.1093/nar/gku293.
Goddard, T.D., Huang, C.C., Meng, E.C., Pettersen, E.F., Couch, G.S., Morris, J.H., Ferrin, T.E., 2018. UCSF ChimeraX: Meeting modern challenges in visualization and analysis. Protein Sci. 27, 14–25. https://doi.org/10.1002/pro.3235.
Goossens, N., Negro, F., 2014. Insulin resistance, non-alcoholic fatty liver disease and hepatitis C virus infection. Rev. Recent. Clin. Trials. 9, 204–209.
Guedes, I.A., de Magalhães, C.S., Dardenne, L.E., 2014. Receptor–ligand molecular docking. Biophys. Rev. 6, 75–87. https://doi.org/10.1007/s12551-013-0130-2.
Hopkins, A.L., 2007. Network pharmacology. Nat. Biotechnol. 25, 1110–1111. https://doi.org/10.1038/nbt1007-1110.
Irshad, M., Gupta, P., Irshad, K., 2017. Molecular basis of hepatocellular carcinoma induced by hepatitis C virus infection. World J. Hepatol. 9, 1305 10.4254%2Fwjh.v9.i36.1305.
Józefiak, A., Larska, M., Pomorska-Mól, M., Ruszkowski, J.J., 2021. The IGF-1 signaling pathway in viral infections. Viruses. 13, 1488. https://doi.org/10.3390/v13081488.
Kuhn, M., von Mering, C., Campillos, M., Jensen, L.J., Bork, P., 2007. STITCH: interaction networks of chemicals and proteins. Nucleic Acids Res. 36, D684–D688. https://doi.org/10.1093/nar/gkm795.
Ladd, A., Duarte, S., Sahin, I. & Zarrinpar, A. Mechanisms of drug resistance in hepatocellular carcinoma. Hepatology, 10.1097. https://doi.org/10.1097/HEP.0000000000000237.
Li, D., Zhang, Y., Liu, K., Zhao, Y., Xu, B., Xu, L., Tan, L., Tian, Y., Li, C., Zhang, W., 2017. Berberine inhibits colitis-associated tumorigenesis via suppressing inflammatory responses and the consequent EGFR signaling-involved tumor cell growth. Lab. Invest. 97, 1343–1353. https://doi.org/10.1038/labinvest.2017.71.
Liu, K.-J., Lv, Y.-X., Niu, Y.-M., Bu, Y., 2020. Prognostic value of γ-glutamyl transpeptidase to albumin ratio combined with aspartate aminotransferase to lymphocyte ratio in patients with hepatocellular carcinoma after hepatectomy. Medicine 99 10.1097%2FMD.0000000000023339.
Luo, D., Tong, J.-B., Zhang, X., Xiao, X.-C., Bian, S.J., 2022. Computational strategies towards developing novel SARS-CoV-2 Mpro inhibitors against COVID-19. J. Mol. Struct. 1247,. https://doi.org/10.1016/j.molstruc.2021.131378 131378.
Magalhães, D., Dos Santos, J., Frutuoso, A., Mesquita, A., Dos Santos, J., Frutuoso Sr, A., 2023. Human Epidermal Growth Factor Receptor 2 (HER2) Expression by Immunohistochemistry and Its Clinical Significance in Hepatocellular Carcinoma: A Single-Center Analysis. Cureus 15. https://doi.org/10.7759/cureus.34724.
Mahmoudvand, S., Shokri, S., Taherkhani, R., Farshadpour, F., 2019. Hepatitis C virus core protein modulates several signaling pathways involved in hepatocellular carcinoma. World J. Gastroenterol. 25, 42 10.3748%2Fwjg.v25.i1.42.
Marrero, J.A., Fontana, R.J., Fu, S., Conjeevaram, H.S., Su, G.L., Lok, A.S., 2005. Alcohol, tobacco and obesity are synergistic risk factors for hepatocellular carcinoma. J. Hepatol 42, 218–224. https://doi.org/10.1016/j.jhep.2004.10.005.
Mohanraj, K., Karthikeyan, B.S., Vivek-Ananth, R., Chand, R., Aparna, S., Mangalapandi, P., Samal, A., 2018. IMPPAT: a curated database of Indian medicinal plants, phytochemistry and therapeutics. Sci. Rep. 8, 1–17. https://doi.org/10.1038/s41598-018-22631-z.
Nakamura, K., Shimura, N., Otabe, Y., Hirai-Morita, A., Nakamura, Y., Ono, N., Ul-Amin, M.A., Kanaya, S.J.P., Physiology, C., 2013. KNApSAcK-3D: a three-dimensional structure database of plant metabolites. Plant Cell Physiol. 54, e4–e. https://doi.org/10.1093/pcp/pcs186.
Needle, D., Lountos, G.T., Waugh, D.S., 2015. Structures of the Middle East respiratory syndrome coronavirus 3C-like protease reveal insights into substrate specificity. Acta Crystallogr D Biol Crystallogr. 71, 1102–1111. https://doi.org/10.1107/S1399004715003521.
Nie, J., Lin, B., Zhou, M., Wu, L., Zheng, T., 2018. Role of ferroptosis in hepatocellular carcinoma. J. Cancer Res. Clin. Oncol. 144, 2329–2337. https://doi.org/10.1007/s00432-018-2740-3.
Noor, F., Rehman, A., Ashfaq, U.A., Saleem, M.H., Okla, M.K., Al-Hashimi, A., AbdElgawad, H., Aslam, S., 2022. Integrating network pharmacology and molecular docking approaches to decipher the multi-target pharmacological mechanism of Abrus precatorius L. acting on diabetes. Pharmaceuticals. 15, 414. https://doi.org/10.3390/ph15040414.
Paskeh, M.D.A., Ghadyani, F., Hashemi, M., Abbaspour, A., Zabolian, A., Javanshir, S., Razzazan, M., Mirzaei, S., Entezari, M., Goharrizi, M.A.S.B., 2022. Biological function and therapeutic perspective of targeting PI3K/Akt signaling in hepatocellular carcinoma: promises and challenges. Pharmacol Res 106553. https://doi.org/10.1016/j.phrs.2022.106553.
Pettersen, E.F., Goddard, T.D., Huang, C.C., Couch, G.S., Greenblatt, D.M., Meng, E.C., Ferrin, T.E., 2004. UCSF Chimera—a visualization system for exploratory research and analysis. J. Comput. Chem. 25, 1605–1612. https://doi.org/10.1002/jcc.20084.
Poustchi, H., Sepanlou, S.G., Esmaili, S., Mehrabi, N., Ansarymoghadam, A., 2010. Hepatocellular carcinoma in the world and the middle East. Middle East J. Dig. Dis. 2, 31.
Qu, C., Wang, Y., Wang, P., Chen, K., Wang, M., Zeng, H., Lu, J., Song, Q., Diplas, B.H., Tan, D., 2019. Detection of early-stage hepatocellular carcinoma in asymptomatic HBsAg-seropositive individuals by liquid biopsy. Proc. Natl. Acad. Sci. 116, 6308–6312. https://doi.org/10.1073/pnas.1819799116.
Rahman, M.A., Mossa, J.S., Al-Said, M.S., Al-Yahya, M.A., 2004. Medicinal plant diversity in the flora of Saudi Arabia 1: a report on seven plant families. Fitoterapia 75, 149–161. https://doi.org/10.1016/j.fitote.2003.12.012.
Shannon, P., Markiel, A., Ozier, O., Baliga, N.S., Wang, J.T., Ramage, D., Amin, N., Schwikowski, B., Ideker, T., 2003. Cytoscape: a software environment for integrated models of biomolecular interaction networks. Genome Res. 13, 2498–2504 10.1101/gr.1239303.
Sher, H., Al-Yemeni, M., Masrahi, Y.S., Shah, A.H., 2010. Ethnomedicinal and ethnoecological evaluation of Salvadora persica L.: a threatened medicinal plant in Arabian Peninsula. J Med Plants Res 4, 1209–1215. https://doi.org/10.5897/JMPR10.230.
Shi, C., Kwong, D.-L.-W., Li, X., Wang, X., Fang, X., Sun, L., Tang, Y., Guan, X.-Y., Li, S.-S., 2022. MAEL Augments Cancer Stemness Properties and Resistance to Sorafenib in Hepatocellular Carcinoma through the PTGS2/AKT/STAT3 Axis. Cancers 14, 2880. https://doi.org/10.3390/cancers14122880.
Smith, B.D., Morgan, R.L., Beckett, G.A., Falck-Ytter, Y., Holtzman, D., Teo, C.-G., Jewett, A., Baack, B., Rein, D.B., Patel, N., 2012. Recommendations for the identification of chronic hepatitis C virus infection among persons born during 1945–1965. Morb. Mortal. Wkly. Rep. 61, 1–32.
Studio, D.J.A., 2008. Discovery studio. Accelrys.
Suresh, D., Srinivas, A.N., Kumar, D.P., 2020. Etiology of hepatocellular carcinoma: special focus on fatty liver disease. Front Oncol. 10,. https://doi.org/10.3389/fonc.2020.601710 601710.
Thrift, A.P., El-Serag, H.B., Kanwal, F., 2017. Global epidemiology and burden of HCV infection and HCV-related disease. Nat Rev Gastroenterol Hepatol. 122–132. https://doi.org/10.1038/nrgastro.2016.176.
Tian, W., Chen, C., Lei, X., Zhao, J. & Liang, J. 2018. CASTp 3.0: computed atlas of surface topography of proteins. Nucleic acids Res. 46, W363-W367. https://doi.org/10.1093/nar/gky473.
Von Mering, C., Jensen, L. J., Snel, B., Hooper, S. D., Krupp, M., Foglierini, M., Jouffre, N., Huynen, M. A. & Bork, P. J. N. a. r. 2005. STRING: known and predicted protein–protein associations, integrated and transferred across organisms. Nucleic acids Res. 33, D433-D437. https://doi.org/10.1093/nar/gki005.
Wang, X., Zhang, A., Sun, H., 2013. Power of metabolomics in diagnosis and biomarker discovery of hepatocellular carcinoma. Hepatology 57, 2072–2077. https://doi.org/10.1002/hep.26130.
Williams-Noonan, B.J., Yuriev, E., Chalmers, D.K., 2018. Free energy methods in drug design: prospects of "alchemical perturbation" in medicinal chemistry: miniperspective. J. Med. Chem. 61, 638–649. https://doi.org/10.1021/acs.jmedchem.7b00681.
Yuan, S., Chan, H.S., Hu, Z., 2017. Using PyMOL as a platform for computational drug design. Wiley Interdiscip. Rev. Comput. Mol. 7, e1298.
Zhang, J., Gao, S., Li, H., Cao, M., Li, W., Liu, X., 2021. Immunomodulatory effects of selenium-enriched peptides from soybean in cyclophosphamide-induced immunosuppressed mice. Food Sci Nutr. 9, 6322–6334. https://doi.org/10.1002/fsn3.2594.
Zhang, X., Li, N., Zhu, Y., Wen, W., 2022. The role of mesenchymal stem cells in the occurrence, development, and therapy of hepatocellular carcinoma. Cancer Med. 11, 931–943. https://doi.org/10.1002/cam4.4521.
Zoete, V., Cuendet, M.A., Grosdidier, A., Michielin, O., 2011. SwissParam: a fast force field generation tool for small organic molecules. J. Comput. Canc. 32, 2359–2368. https://doi.org/10.1002/jcc.21816.
Zou, Z., Tao, T., Li, H., Zhu, X., 2020. mTOR signaling pathway and mTOR inhibitors in cancer: Progress and challenges. Cell Biosci. 10, 1–11. https://doi.org/10.1186/s13578-020-00396-1.